Frequency-dependent dynamics of domain walls in yttrium iron garnet

C. Torres,* Ó. Alejos, J. M. Muñoz, P. Hernández-Gómez, and C. de Francisco
Departamento Electricidad y Electronica, Facultad de Ciencias, Universidad de Valladolid, 47071 Valladolid, Spain
(Received 18 October 2001; revised manuscript received 17 January 2002; published 28 June 2002)

An analysis of the frequency-dependent dynamics of domain walls in polycrystalline yttrium iron garnet samples is presented. This analysis has been carried out, on the one hand, considering the theoretical aspects related to the numerical solving of the motion of a Bloch wall using harmonic fields. On the other hand, we have measured the magnetic aftereffect phenomena by using the technique known as magnetic disaccommodation. The experimental results change drastically with the measuring frequency for all the samples, showing the presence of a relaxing process related to the electronic hopping between ferric and ferrous ions and magnetic accommodation processes. The agreement between these results and the theoretical model analyzed has led us to interpret these phenomena in terms of a time-dependent resonance mechanism when an induced anisotropy relaxing process takes place.

DOI: 10.1103/PhysRevB.66.024410 PACS number(s): 76.60.Es, 75.50.Gg

I. INTRODUCTION

In a preceding paper[1] we dealt with the problem of the frequency-dependent dynamics of domain walls in magnetically ordered materials when magnetic aftereffects (MAE's) appear. This processes are highly undesirable from a technical point of view as they mean a delayed change in magnetization after a variation in the magnetic field; thus they represent an important source of magnetic losses in these materials. However, they are very useful for basic research as they provide important information about lattice symmetry and dynamics. In fact, according to the model first proposed by Néel,[2] they have their origin in the relaxation of the induced magnetic anisotropy due to a redistribution of magnetic dipoles into the lattice. The analysis of MAE's is usually carried out by means of magnetic disaccommodation (DA) techniques, which consist of the measurement of the time evolution of the magnetic initial permeability of a sample after demagnetization. These techniques have been widely applied to different ferromagnetic materials as magnetite,[3–6] single spinel ferrites with different substitutions,[7–12] hexagonal ferrites,[13,14] and garnets.[15–20] In the case of yttrium iron garnet (YIG) these kinds of measurements have proven the existence of ferrous ions in the lattice due to an oxygen deficient structure, confirming the similar conclusions obtained in other kinds of experiments such as electric conductivity,[21] rotational hysteresis,[22] or domain-wall mobility.[23] Nevertheless, a very different behavior has been checked in the case of YIG in relation to other kind of ferrites: the appearance of negative magnetic disaccommodation processes, to which we will refer as accommodation processes. These phenomena, which are characterized by an increase of the initial permeability with time, are still an open question in the sense that none of the models proposed have provided a complete understanding of the underlying mechanisms. In a recent work[20] we showed the critical dependence of these processes on the measuring frequency. For these reasons, in this paper we first explain the main conclusions of our theoretical model concerning the frequency-dependent dynamics of domain walls. Then we describe the method utilized for the fabrication of the samples and for the DA measurements. Finally, after a complete analysis of the experimental results and their extreme dependence on the frequency, a detailed discussion of these results is carried out. The comparison between the theoretical model and the experimental results obtained from our measurements have led us to make very important assumptions about the nature of the magnetic accommodation processes. Concretely, we have associated these processes with a resonance phenomenon whose features depend on time due to the presence of an induced anisotropy relaxation process.

II. THEORETICAL BACKGROUND

In accordance with the model proposed by Néel, it can be considered that the motion of a Bloch wall under the influence of an applied magnetic field, possibly time dependent, is defined by the sum of different stresses. The first of these is the stress due to the applied magnetic field. The second is an elastic term that refers the wall to its equilibrium position, and is associated with lattice internal stresses, dislocations, etc. Another one, proportional to the wall speed, takes account of damping effects that prevent a free wall oscillation after a change in its position. Finally, we must consider a stress due to the redistribution of magnetic dipoles within the lattice. Hence the dynamic equation for the Bloch wall can be expressed as

$$m\ddot{u}+v\dot{u}=-R(u)+\vec{H}(t)(\vec{M}_2-\vec{M}_1)+P(u,t), \qquad (1)$$

where u is the wall instantaneous position, m is the wall inertial mass, v is the damping coefficient, $-R(u)$ is an elastic term, and $\vec{M}_1$ and $\vec{M}_2$ are the values of the magnetization on each side of the wall. The redistribution stress $P(u,t)$ is obtained by computing the instantaneous anisotropy energy associated with a unity surface of the wall considering the lattice symmetry and the directions of the magnetizations $\vec{M}_1$ and $\vec{M}_2$. This stress consists of two terms,[1,24] the first related to magnetic aftereffects in the material and the second to the magnetic viscosity. However, this second term vanishes when the initial state of the material is given by a demagnetized state,[1] that is, when the directions of the magnetic di-

 ©2002 The American Physical Society

poles inside the material are equally distributed. This is precisely the case in our theoretical and experimental study, which allows us to analyze in detail the magnetically induced anisotropy relaxation and then the aftereffect phenomena in these materials. Therefore, the redistribution stress can be written as

$$P(u,t) = -P_0 \int_0^t f[u(t') - u(t)] g(t-t') dt', \qquad (2)$$

$f(U)$ being a function of the difference of the instantaneous positions of the wall at two different time instants that depends on the wall type.[25] Then this stress refers the wall to all of its previous positions, but is weighted by the function $g(t)$. This function is strictly decreasing and is defined by

$$g(t) = \int_0^\infty \frac{p(\tau)}{\tau} e^{-t/\tau} d\tau, \qquad (3)$$

$p(\tau)$ being the probability of a relaxation process of time constant τ. As can be expected, the stress due to the immediately preceding positions is the most important in the weighting.

At this moment, some reasonable approximations must be made in order to simplify the solution of Eq. (1). If we consider that the wall motion stays in the zone where the $R(u)$ function is approximately linear and write the magnetic field stress as proportional to its modulus and to the saturation magnetization, we obtain

$$m\ddot{u} + v\dot{u} = -ru + \gamma H(t) M_s + P(u,t). \qquad (4)$$

However, the term due to the induced anisotropy relaxation makes it difficult to solve the dynamic equation of the wall motion. For this reason, some authors[26] proposed solutions by means of an attraction between the wall and some mobile elements, which act as pinning centers, that is used instead of the $P(u,t)$. This study can also be carried out taking into account that the wall displacements are also in the linear zone of the $f(U)$ function, as in the case of the elastic term. Then $f(U) \cong -fU$, f being a constant, and therefore we can write

$$m\ddot{u} + v\dot{u} = -ru + \gamma H(t) M_s - fP_0 \left[u(t) G(t) - \int_0^t u(t') g(t-t') dt' \right], \qquad (5)$$

where we have introduced the relaxing function $G(t)$ given by

$$G(t) = \int_0^t g(t') dt' = 1 - \int_0^\infty e^{-t/\tau} p(\tau) d\tau, \qquad (6)$$

which increases from $G(0)=0$ to $G(\infty)=1$. In a simple case, $G(t)$ presents multiexponential features, but depends on the applied model for the relaxation. In some cases, there are experimental relaxation results that require a description by means of another kind of function as the stretched exponential.[27]

In order to obtain the approximate solution of Eq. (5) we will consider two different situations. First, when the applied magnetic field has a very low frequency ω, it can be supposed that the inertial and damping terms of Eq. (5) are negligible, and then this is no longer a differential equation. Depending on the $\omega\tau$ product, different situations can take place. When $\omega\tau \ll 1$, the redistribution of the magnetic dipoles is fast enough to keep the system in equilibrium. On the other hand, if the magnetic field has a frequency given by the inverse of the time constant τ, that is, $\omega\tau = 1$, the wall motion will be damped by the magnetically induced anisotropy relaxation, although the displacements tend to remain near the wall equilibrium position. As the frequency increases the redistribution effect will modulate the wall motion, modifying its speed. Therefore, the frequency spectrum of the wall response $u(t)$ spreads slightly, especially near the field frequency ω. Finally, when the time constants of the redistribution are greatly above the inverse of the field frequency, that is, $\omega\tau \gg 1$, the function $g(t-\theta)$ acts as a low-pass filter in the convolution term given by $\int_0^t u(\theta) g(t-\theta) d\theta$, and hence this term vanishes. Taking into account these considerations, we can write the solution of Eq. (5) as

$$u(t) \simeq \frac{\gamma M_s}{r[1 + \eta G(t)]} H(t), \qquad (7)$$

where we have introduced the parameter $\eta = fP_0/r$, which defines the ratio between the elastic constant r and another elastic term added by the induced anisotropy relaxation term. When $\eta \gg 1$ this second term prevails. Hence, if $\omega\tau \gg 1$, the wall mobility decreases with time and the magnetic susceptibility $\chi(t)$ will decrease too, if we take into account that

$$\chi(t) \propto \frac{u(t)}{H(t)} \simeq \frac{\gamma M_s}{r[1 + \eta G(t)]}. \qquad (8)$$

This situation is the most frequently detected in this kind of experimental measurements carried out with the majority of magnetic materials, giving rise to the phenomena known as magnetic disaccommodation. Figure 1 presents the wall frequency response for a constant value of $\eta = 5$, sufficiently high to take account of the induced anisotropy relaxation phenomena.

Now let us suppose that we apply a high-frequency magnetic field. In this case, the inertial and damping terms of Eq. (5) cannot be neglected. However, using the same approximation as in obtaining Eq. (7), we can write Eq. (5) as[1]

$$\ddot{u} + 2\delta\omega_n u + \omega_n^2 [1 + \eta G(t)] u = u_0 \omega_n^2 \sin \omega t, \qquad (9)$$

$\omega_n = \sqrt{(r/m)}$ being the wall natural resonance frequency, $\delta = v/2\omega_n m$ the damping coefficient, and $u_0 = \gamma M_s H_0 / r$. This differential equation can be solved numerically.[1,24] Depending on the values of δ and ω the wall amplitude can show different dependences on time, and so it can increase initially, pass through a maximum, and then decrease. This anomalous behavior can be interpreted as a time-dependent

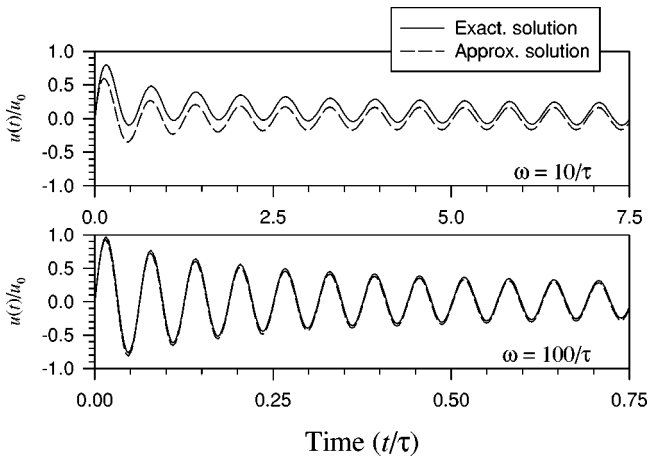

FIG. 1. Wall response under the action of a harmonic magnetic field for different frequencies and a sufficiently high value of η (see the text).

wall resonance. In fact, since we are considering second-order wall dynamics, the relaxation term will increase with time, so that the elastic term will be also increased. As a consequence, the wall resonance frequency will increase with time as

$$\omega_0 = \omega_n \sqrt{1+\eta G(t)}. \tag{10}$$

The transients caused by this time variation will vanish if it is sufficiently slow, and, thus, it is possible to obtain an approximate solution for the wall response given by

$$|u(t)| \simeq \frac{u_0}{\sqrt{\left[1-\frac{\omega^2}{\omega_n^2}+\eta G(t)\right]^2+4\delta^2\frac{\omega^2}{\omega_n^2}}}. \tag{11}$$

The evolution of the wall frequency response is shown in Fig. 2. It can be noted that the resonance peak is more relevant for increasing time values. Thus, depending on the field frequency (and, of course, of the initial damping coefficient), the wall oscillation amplitude will either decrease, increase, or both with time (ω_1, ω_3, or ω_2 in the figure, respectively).

III. EXPERIMENTAL PROCEDURE

A. Sample preparation

A set of polycrystalline samples with nominal composition $Y_3Fe_{5-x}O_{12}$ was prepared by mixing high purity Fe_2O_3 and Y_2O_3 powders in the appropriate molar ratio. The mixture was ground and pressed in a cylindrical die at 10000 kg/cm^2. The resulting green samples, 5 mm in diameter and 15 mm in length, were fired at different temperatures and partial oxygen pressures according to the corresponding phase diagrams.[28] Finally, rapid quenching in the furnace was performed to avoid possible vacancy annealing. X-ray powder diffraction patterns of these samples showed that single-phase YIG was obtained for each composition.

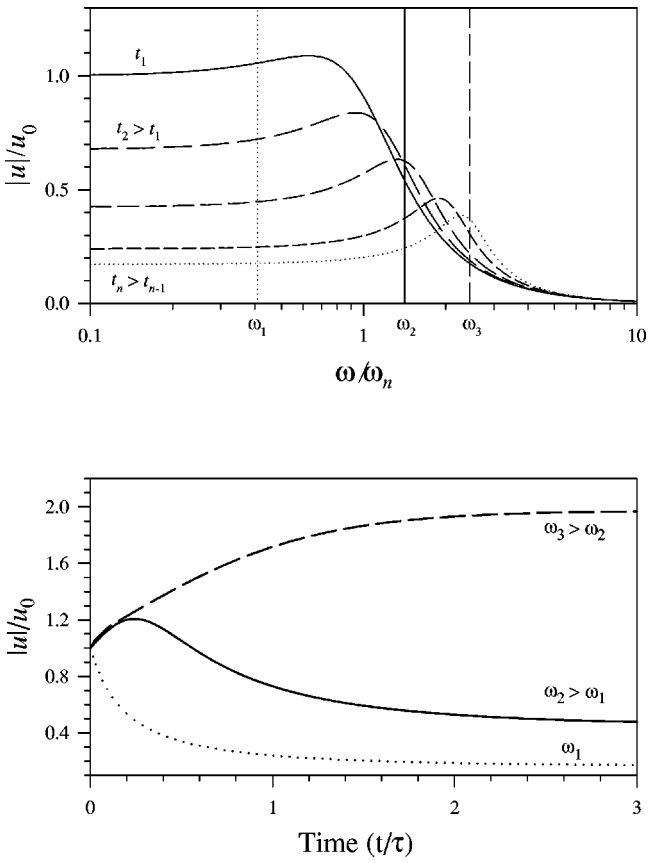

FIG. 2. Time evolution of the frequency wall response and instantaneous amplitude obtained for a given high-frequency magnetic field.

B. Measurement technique

Magnetic disaccommodation measurements have been carried out with the help of a computer-aided system based on an automatic impedance (LCR) meter.[29] During the measuring process, the time variations of both the real and imaginary components of the initial magnetic permeability was recorded at different temperatures. The measuring coil was excited by a low amplitude (≈ 2 Oe) sinusoidal signal with frequency ranging from 200 Hz to 4 kHz. Samples were demagnetized by using a low-frequency decreasing alternating field whose characteristics (peak amplitude, frequency and total duration) were checked in order to obtain coherent disaccommodation results.[29]

DA results are usually represented by means of the isochronal curves displaying the relative variation of permeability within different time windows,

$$\mathrm{DA}(\%) = \frac{\mu(t_1,T)-\mu(t_2,T)}{\mu(t_1,T)} \times 100, \tag{12}$$

where the different curves displayed have been obtained in our case using $t_1 = 2$s and $t_2 = 4$, 8, 16, 32, 64 and 128 s after demagnetization stage. When the time window $(t_2 - t_1)$ is of the same order of magnitude as the relaxation time at a specific temperature, this curve exhibits a maximum. Isochronal

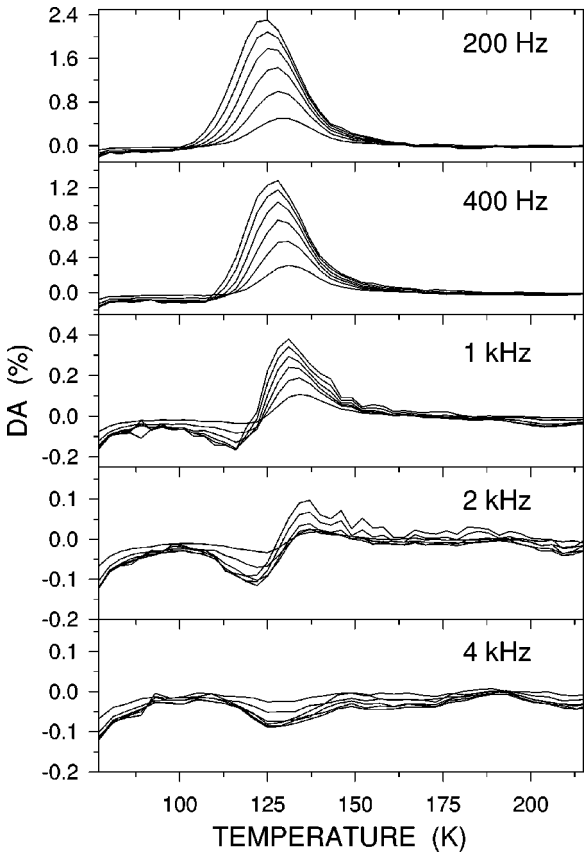

FIG. 3. Isochronal relaxation spectra at different measurement frequencies for a YIG sample with nominal composition $3Y_2O_3 + 5Fe_2O_3$ sintered in CO_2 at 1420 °C.

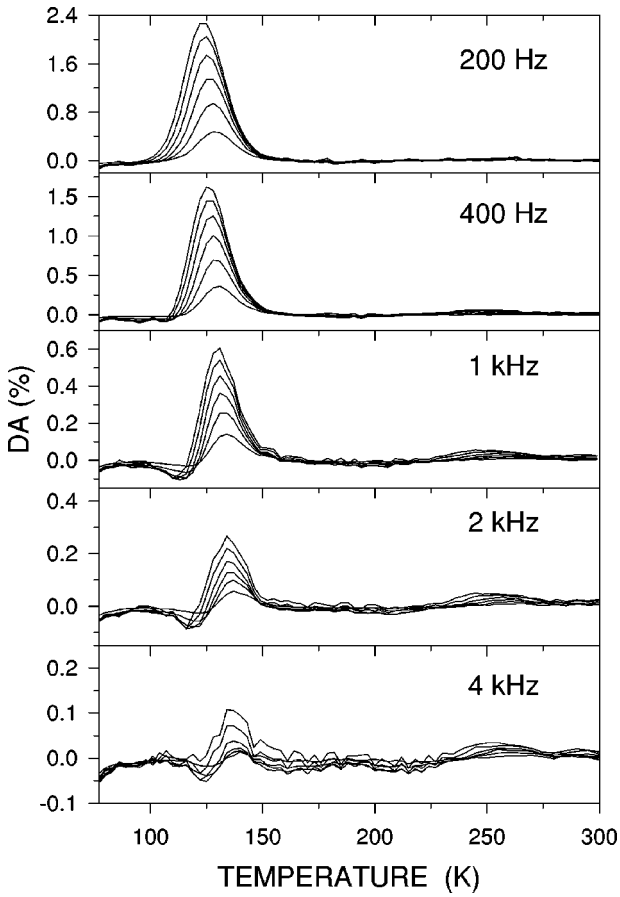

FIG. 4. Isochronal relaxation spectra at different measurement frequencies for a YIG sample with a nominal composition $3Y_2O_3 + 4.9Fe_2O_3$ sintered in CO_2 at 1420 °C.

curves are very useful in our study because they allow us to distinguish the various thermal relaxation processes.

IV. EXPERIMENTAL RESULTS

Figure 3 shows the permeability isochronal spectra measured at different frequencies for a YIG sample with nominal composition $3Y_2O_3 + 5Fe_2O_3$ sintered in CO_2 at 1420 °C. It can be noted the presence of the well-known process II,[18,30] with its maximum around 125 K for a frequency of 200 Hz. Simultaneously, an accommodation (or negative disaccommodation) process appears at temperatures just below process II, as reported only in the case of garnets sintered under reducing conditions[15,16] as in this case. However, the most important characteristic of these spectra is their critical dependence on the measurement frequency, a phenomenon never detected previously in similar experiments carried out with other kind of ferrites, to our knowledge. As this frequency is increased, two phenomena take place. First, the negative and the positive processes seem to ''overlap,'' so that the ratio between the amplitudes of both peaks decreases gradually (for example, they become very similar for 2 kHz). Second, the maxima of both processes shift to higher temperatures, and, as consequence, the transition temperature for which every isochronal DA spectrum passes through zero increases too. Finally, process II can hardly be detected at 4 kHz and the accommodation peak results centered around 125 K.

The corresponding isochronal relaxation spectra obtained for YIG samples sintered in the same conditions but with a slight defect or excess of iron oxide in their initial composition are represented in Figs. 4 and 5 respectively. The behavior detected is very similar to the above analysis, so that the small modifications achieved do not produce relevant variations in the disaccommodation curves. It can be mentioned that the accommodation peak is slightly weaker for the sample with a defect of iron in its nominal composition. Finally, a similar experiment was carried out but, in this case, changing the sintering conditions of the samples. First we have fired a sample in an atmosphere given by a fixed mixture of air and helium in the appropriate ratio so that a less reducing atmosphere than CO_2 is obtained (in particular with a partial oxygen pressure of 10^{-2} atm). The results are displayed in Fig. 6, and show a very similar behavior to that obtained using CO_2 as sintering atmosphere. It can be noted that the DA process II, as well as the accommodation processes, occurs on the contrary to the air sintering atmosphere.[15,18,31] Second, we increased the sintering temperature up to 1450 °C. The corresponding relaxation isochronal curves can be examined in Fig. 7. In this case, process II and the accommodation peak are again detected,

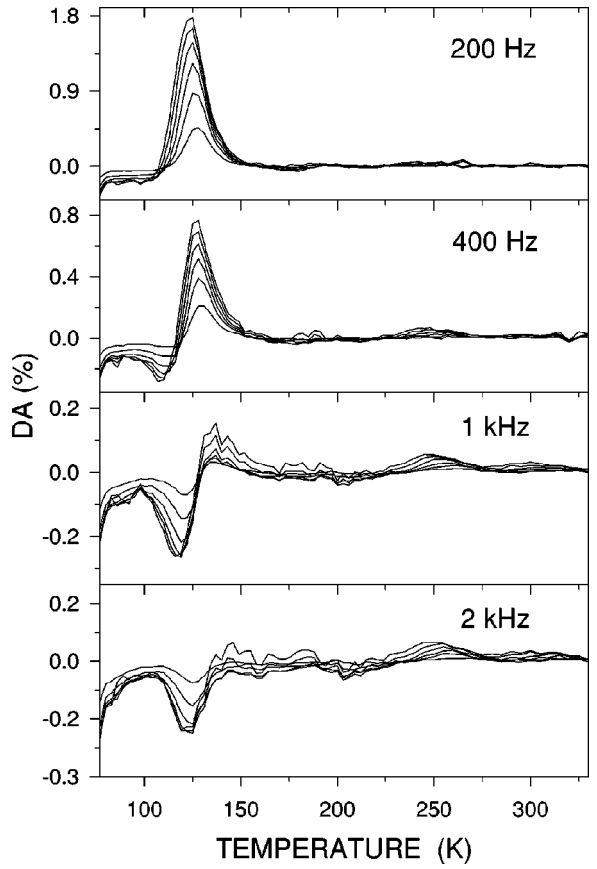

FIG. 5. Isochronal relaxation spectra at different measurement frequencies for a YIG sample with a nominal composition $3Y_2O_3 + 5.1Fe_2O_3$ sintered in CO_2 at 1420 °C.

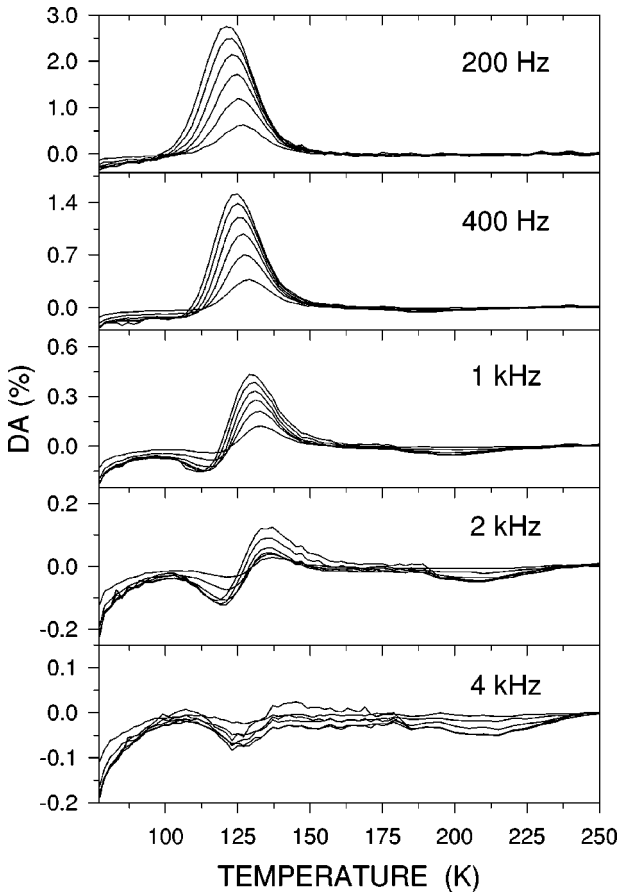

FIG. 6. Isochronal relaxation spectra with different measurement frequencies for a YIG sample with a nominal composition $3Y_2O_3 + 5Fe_2O_3$ sintered at 1420 °C in an atmosphere of air/helium with a partial oxygen pressure of 10^{-2} atm.

showing the same dependence on the increasing measurement frequency. However, it can be noted that a DA process appears at temperatures around 187 K. As opposed to process II, the features of this peak do not depend on the measurement frequency. A reduction of its amplitude can be only detected at the highest frequencies, which is due to the worsening of the signal-to-noise ratio in the measurement equipment.

On the other hand, in Fig. 8 we plot the thermal evolution of the relative initial magnetic permeability (at different values of the frequency) measured 2 and 128 s after the demagnetization stage in order to confirm the existence of relaxing processes. In addition, we display not only the real part of the permeability, as is typical, but also the imaginary part. The aim of this strategy is related to the theoretical ideas exposed in Sec. II. In fact, if a resonance phenomenon takes place, this imaginary part, associated with the magnetic losses of the material, must change significantly.

The results obtained in this way for the YIG sample with stoichiometric composition are presented in Fig. 8. It can be observed that the real part of the permeability [Fig. 8(a)] increases with temperature showing two local maxima that shift to greater temperatures as the measurement frequency is increased. Thus, the first of them, much more relevant, is located at 125 K for 200 Hz and around 165 K for 4 kHz, while the second moves from 200 to 235 K for the same frequency range. However, there is an essential difference between them that consists of a marked variation of the first maximum with the measuring time that does not occur in the second maximum. This phenomenon is especially pronounced for the lowest frequencies and is considered to be due to a relaxing process. Indeed, the corresponding isochronal curves (Fig. 3) show this process (called process II) at the same temperatures for each frequency.

Figures 8(b)–8(e) display the thermal evolution of the imaginary part of the magnetic permeability of this sample at different measurement frequencies. The presence of two maxima can again be detected. These maxima shift to higher temperatures with increasing frequencies. However, two important conclusions result noticeable. First, these maxima occur at temperatures slightly lower (around 15 K) than their equivalents in the real part. Second, the behavior of both is very different if the time passed from the demagnetization stage is considered. Thus the temperature and intensity of this first peak depend radically on this time, in contrast to the second that does not vary significantly with it. When the measuring frequency is increased the magnetic losses of the material are greater, thus avoiding the detection of these phenomena so clearly.

A similar study was developed for the rest of the samples sintered in our laboratory. Thus we have confirmed that the small variations in the initial composition of the samples

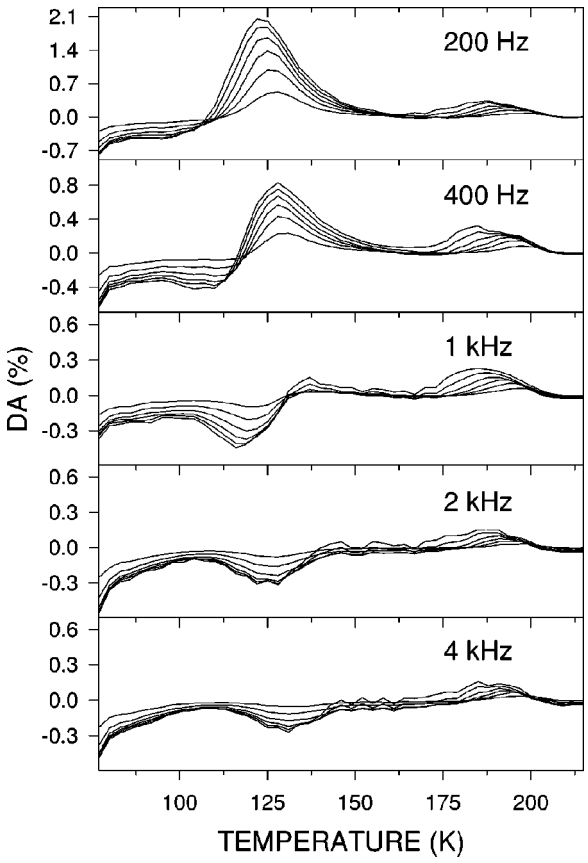

FIG. 7. Isochronal relaxation spectra at different measurement frequencies for a YIG sample with a nominal composition $3Y_2O_3+5Fe_2O_3$ sintered in CO_2 at 1450 °C.

around the stoichiometric YIG give rise again to very similar results (Figs. 9 and 10). In other words, both parts, real and imaginary, of the initial permeability show the two maxima previously mentioned at similar temperatures, where the first of them varies strongly with the measuring time. Finally, similar results have been obtained by changing the sintering conditions of the samples, as can be seen in Fig. 11 (a sample sintered in an atmosphere with a partial oxygen pressure of 10^{-2} atm) and Fig. 12 (a sample sintered at 1450 °C). It must be mentioned that, in this last case, the peak located near 200 K slightly decreases its amplitude with the measuring time [Fig. 12(a)], which is due to the relaxing process already detected in the magnetic disaccommodation spectra (Fig. 7). It is noteworthy that the samples analyzed in previous works,[15,18,30] which did not show any magnetic accommodation process, presented a very different behavior through these kind of representations. For example, the thermal evolution of both components of the initial permeability for a YIG sample sintered in air at 1420 °C is displayed in Fig. 13. In this case neither the real nor imaginary curves show any local maxima over the entire temperature range tested. It can be pointed out that both curves present a slight decrease with time (see the curves at $t_1=2$ s. and $t_2=128$ s in the figure) at temperatures below 150 K, which is due to the relaxing phenomena detected in the magnetic disaccommodation spectra displayed in those works.

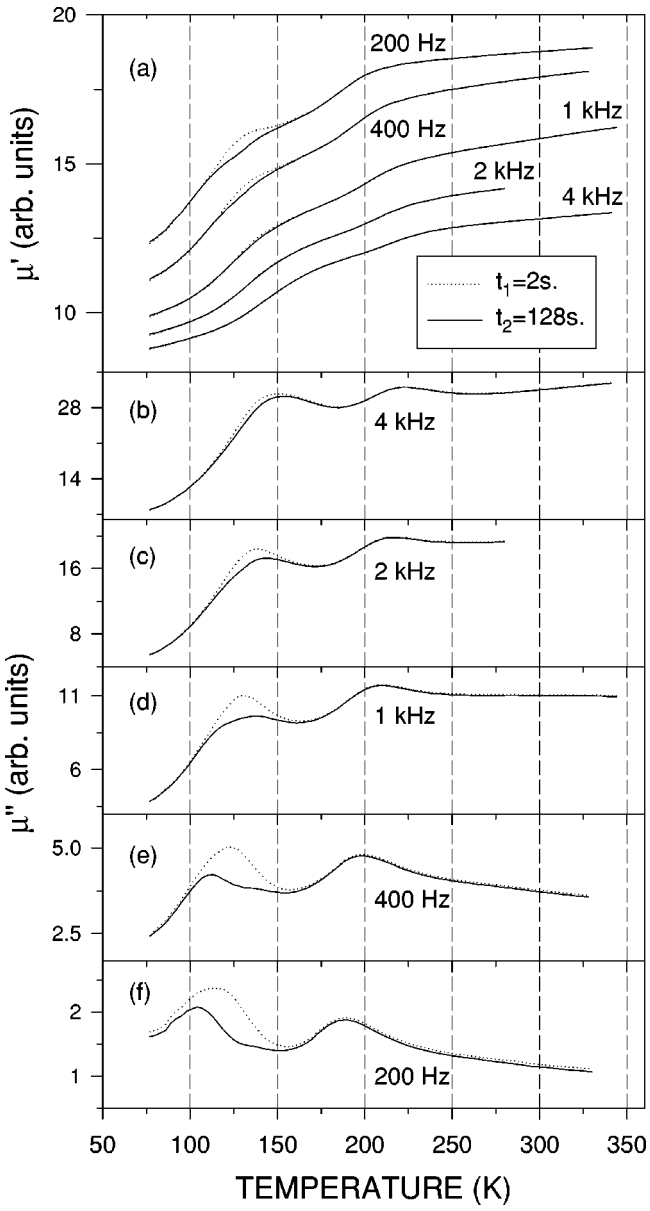

FIG. 8. Relative initial magnetic permeability measured 2 and 128 s after demagnetization at different measurement frequencies for a YIG sample with a nominal composition $3Y_2O_3+5Fe_2O_3$ sintered in CO_2 at 1420 °C [(a) real part; (b)–(f) imaginary part].

V. DISCUSSION

The following discussion requires a previous revision of the characteristics of YIG's and, concretely, of the specific lattice positions. The unit cell of this ferrimagnetic garnet is composed of eight formula units forming a complex cubic lattice constituted by altogether 160 ions. In this crystal there are three groups of trivalent metal ions distributed on fourfold-coordinated tetrahedral *d* sites, sixfold-coordinated octahedral *a* sites, and eightfold-coordinated dodecahedral *c* sites.[32] In the special case of YIG, these *c* sites are occupied by Y^{3+} ions, which are diamagnetic, while the magnetic moments of *a* site ions are oriented antiparallel to those of the *d* positions. In consequence, the magnetic moment per formula unit ($5\mu_B$) is given by the surplus of tetrahedral Fe^{3+} ions.

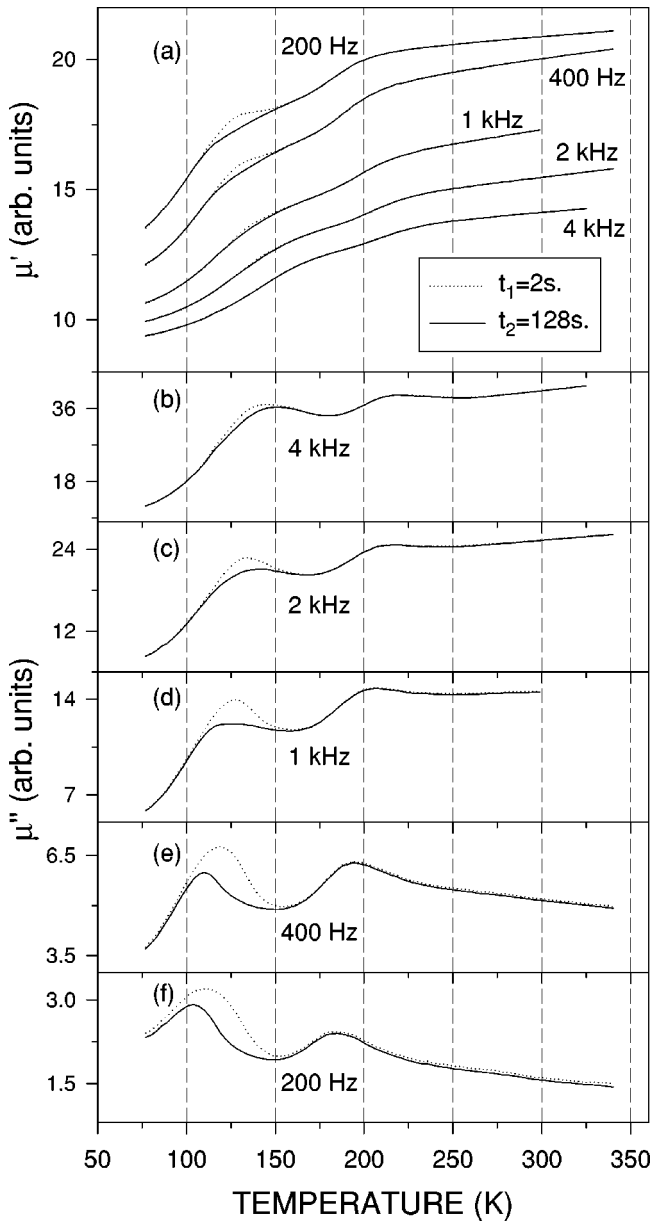

FIG. 9. Relative initial magnetic permeability measured 2 and 128 s after demagnetization at different measurement frequencies for a YIG sample with a nominal composition $3Y_2O_3+4.9Fe_2O_3$ sintered in CO_2 at 1420 °C [(a) real part; (b)–(f) imaginary part].

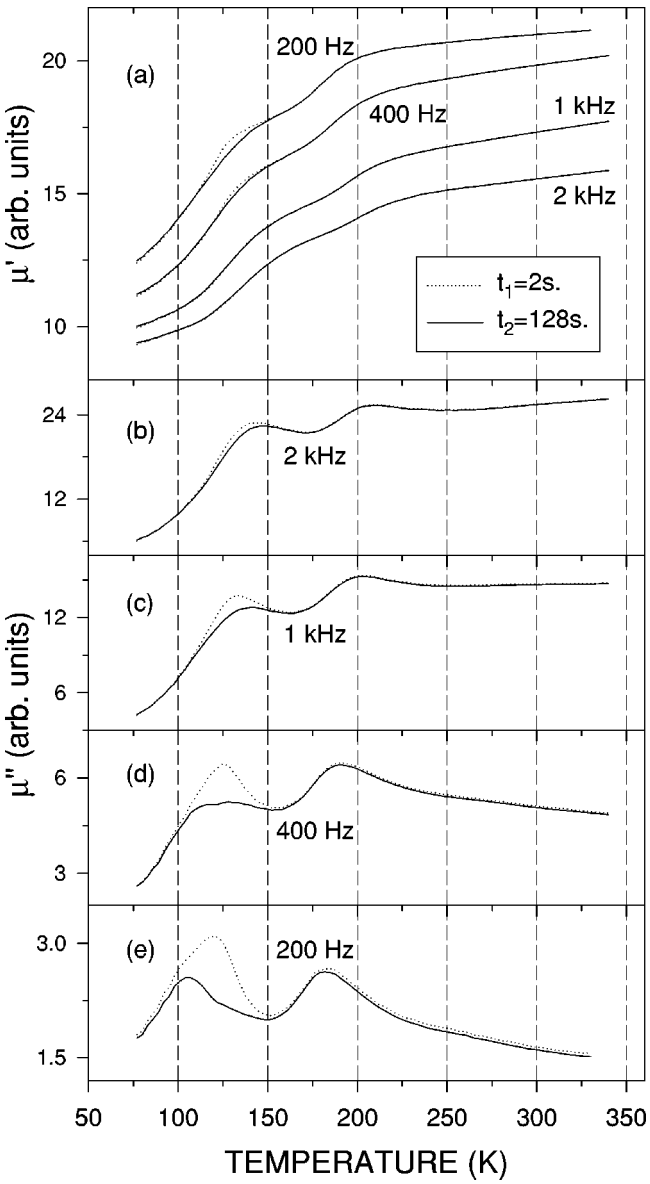

FIG. 10. Relative initial magnetic permeability measured 2 and 128 s after demagnetization at different measurement frequencies for a YIG sample with a nominal composition $3Y_2O_3+5.1Fe_2O_3$ sintered in CO_2 at 1420 °C [(a) real part; (b)–(e) imaginary part].

It has been assumed that this occupancy of the three sublattices by three-valent metal ions may be the origin of the great insulator behavior of these ferrites. Moreover, due to their zero-orbital ground states, $^1S_0$ (Y^{3+}) and $^6S_{5/2}$ (Fe^{3+}), these ions are characterized by a very reduced anisotropy and thus exhibit only weak interactions with other sources of anisotropy in the crystal. Therefore, the mere occurrence of magnetic aftereffect phenomena in our samples, as the magnetic disaccommodation spectra show, is a clear indication of a certain nonstoichiometry in the compound. According to phase diagrams,[28] when preparing high temperature sintered YIG, a slightly oxygen deficient structure appears. In order to maintain charge neutrality in the lattice, this oxygen deficit is compensated for by a corresponding valency change of Fe^{3+} into Fe^{2+} ions. Taking into account their relatives sizes, these ferrous ions are expected to occupy preferentially the wider octahedral sites, although occasionally minor contents of Fe^{2+} ions have been also found on tetrahedral positions. In any case, the assumption of coincident presence of Fe^{3+} and Fe^{2+} ions in our samples enables electron exchange between differently valent Fe ions according to[33]

$$Fe^{3+}+e^-\Leftrightarrow Fe^{2+}. \tag{13}$$

This local electron hopping implies a corresponding transport of local anisotropy onto the site of the ferrous ion which, due to its initial $^5D_4$ state, retains a certain orbital

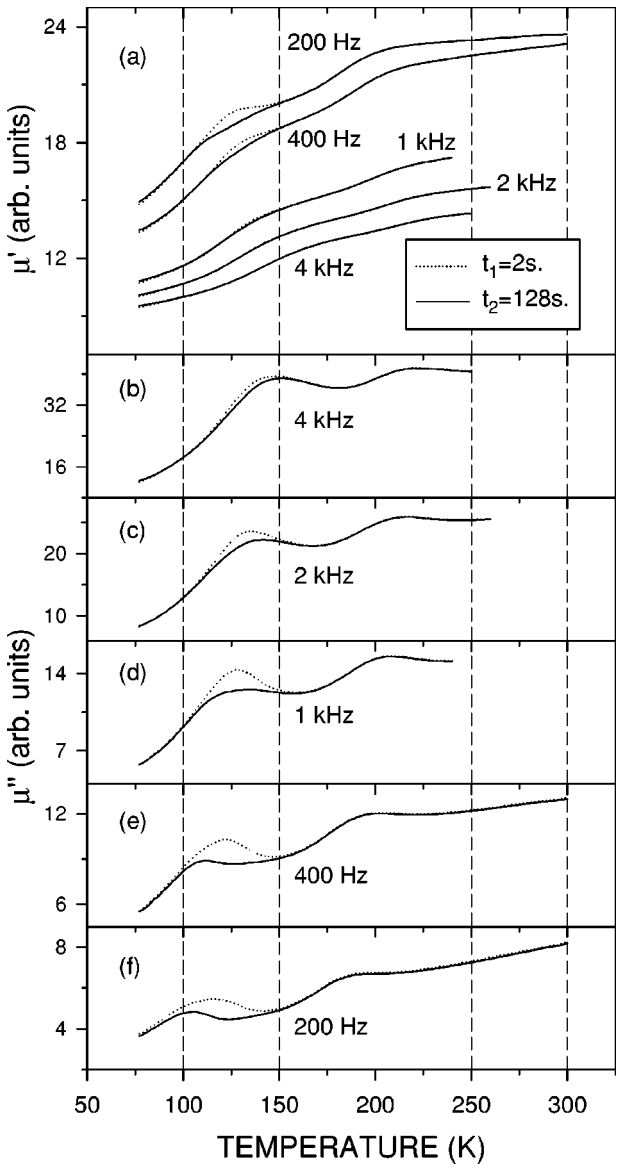

FIG. 11. Relative initial magnetic permeability measured 2 and 128 s after demagnetization at different measurement frequencies for a YIG sample with a nominal composition $3Y_2O_3+5Fe_2O_3$ sintered at 1420 °C in an atmosphere of air/helium with a partial oxygen pressure of 10^{-2} atm [(a) real part; (b)–(f) imaginary part].

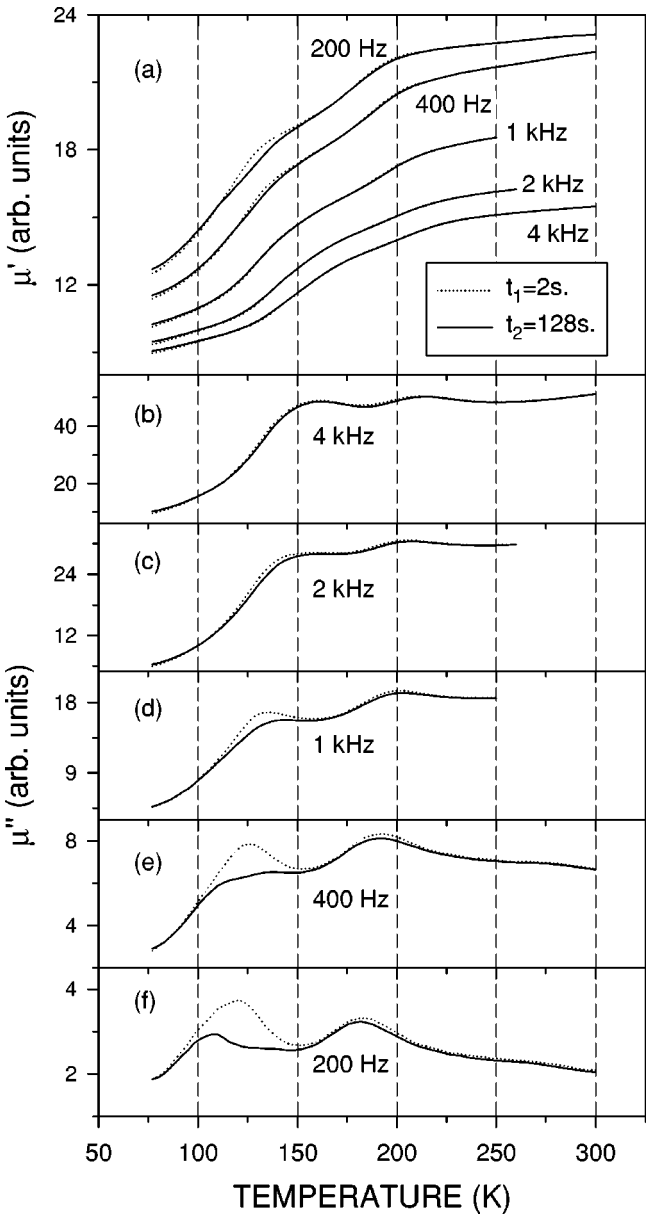

FIG. 12. Relative initial magnetic permeability measured 2 and 128 s after demagnetization at different measurement frequencies for a YIG sample with a nominal composition $3Y_2O_3+5Fe_2O_3$ sintered in CO_2 at 1450 °C [(a) real part; (b)–(f) imaginary part].

momentum in the lattice. Therefore, this valence exchange must be considered as the basic process for magnetic relaxations in undoped YIG.

Concerning the octahedral positions, it must be remembered[34] that the oxygen anions are trigonally disposed around these sites, so that their symmetry axis coincides with one of the [111] axes (Fig. 14). This trigonal field splits the free-ion level into a singlet and two doublets.[21,33,35] Depending on the trigonal field orientation,[33] the ground state will be characterized either by a singlet or a doublet. Moreover, these levels are split into $2S+1$ sublevels due to the exchange interaction. Finally, for an ion such as Fe^{2+} characterized by a not quenched angular momentum ($L\neq 0$), the doublet is further split due to the spin-orbit coupling. Therefore, there are at least four inequivalent types of octahedral positions for the ferrous ion in YIG, each of them having its symmetry axis located at the different [111] axes. In conclusion, it is evident that the distribution of the ferrous ions in the equilibrium state in octahedral positions will depend on the spontaneous magnetization. Thus, after a change of its direction, as happens during the demagnetization stage, a rearrangement of these ions takes place through the electron exchange between Fe^{2+} and Fe^{3+} ions in order to minimize the free enthalpy of the system. These transitions lead to a characteristic immobilization of the domain walls which gives rise to the experimentally observable magnetic aftereffects, i.e., the process found around 130 K, known as process II. Besides this anisotropy, due to the trigonal field, one must also consider the fact that the cubic symmetry is not perfect

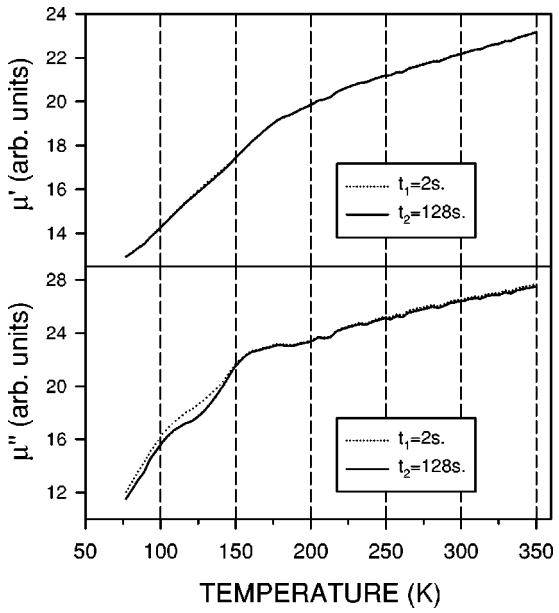

FIG. 13. Relative initial magnetic permeability measured 2 and 128 s after demagnetization at 1 kHz for a YIG sample with a nominal composition $3Y_2O_3+5Fe_2O_3$ sintered in air atmosphere at 1420 °C.

at octahedral positions. Thus the octahedra formed by the oxygen anions around a cation in an *a* site are elongated along the [111] direction, undergoing a trigonal distortion. As a consequence, two energetically inequivalent octahedral positions can be associated with each of the [111] axes just by a rotation about these directions through opposite angles of 28.6°.

At this point, it seems reasonable to suppose that the hopping mechanism between Fe^{3+} and Fe^{2+} in octahedral positions (process II) cannot be related to a simple exponential process. That is to say, for a given octahedral site there are

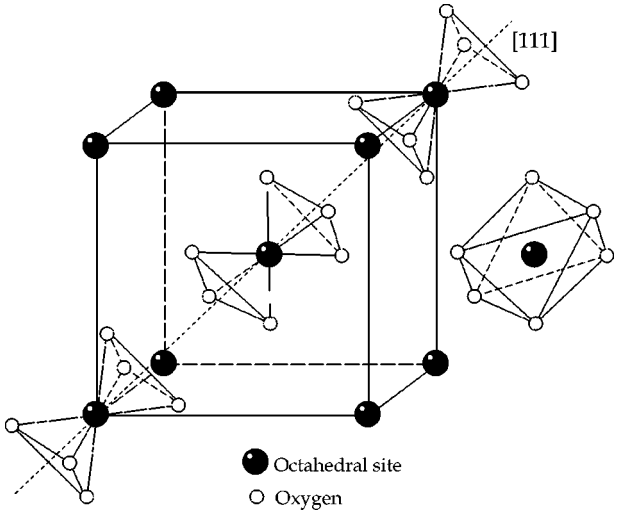

FIG. 14. One-eight unit cell showing the trigonal disposition of the oxygen ions around one of the four [111] symmetry axes. The center site has been duplicated at the right to show the octahedral configuration (Ref. 21).

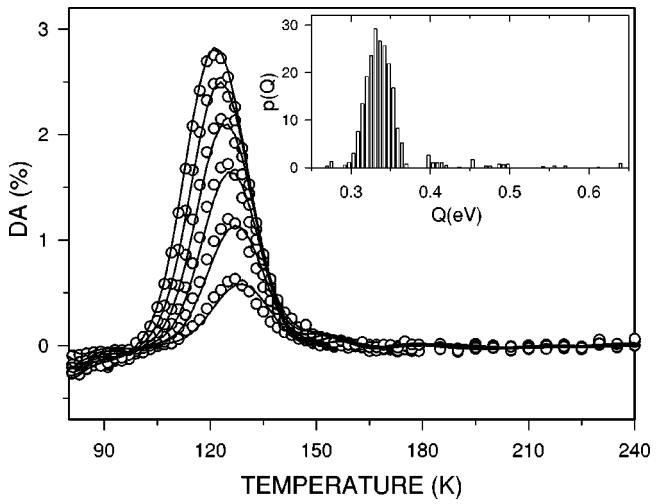

FIG. 15. Experimental DA spectrum (dots) and theoretical fitting (full lines) for the YIG sample sintered at 1420 °C in an atmosphere of air/helium with a partial oxygen pressure of 10^{-2} atm. The inset shows the activation energy spectra obtained by the fitting.

different configurations for the electronic hopping leading to a spread of the energy spectrum, as previously proposed by other authors.[21,22] In fact, in order to fit our isochronal spectra it has been necessary to apply an algorithm developed by our group[30,31] based on the use of an activation energy distribution $p(Q)$, since they cannot be satisfactorily analyzed through a discrete sum of single Debye processes. For example in Fig. 15 we plot the experimental disaccommodation spectrum measured at 200 Hz, together with the mathematical fitting, for a YIG sample sintered at 1420 °C in an atmosphere with a partial oxygen pressure of 10^{-2} atm. The results in this way obtained are very similar for all the samples prepared, and show a quite narrow distribution of energies with values centered around 0.32 eV. Comparable values of these activation energies have been found by other authors not only in analogous measurements of magnetic disaccommodation[18,36] but also in other kinds of measurements such as conductivity,[21,37] variation of tan δ,[38] domain-wall mobility,[23] complex initial permeability,[39,40] or magnetic loss factor.[41]

On the other hand, we have detected another DA process around 187 K when the sintering temperature is increased up to 1450 °C (Fig. 7). Concerning this peak, we must consider, as pointed out above, that sintering conditions are the cause of an oxygen-deficient crystalline structure. As a consequence, one must assume the presence of oxygen vacancies in the lattice, enhanced by lower partial oxygen pressures and higher sintering temperatures. These vacancies behave as positive centers in the lattice, and thus may trap electrons. Therefore, they may appear as neutral (V_O, with two trapped electrons), singly positively charged ($V_O^{\bullet}$, with one trapped electron) and doubly positively charged ($V_O^{\bullet\bullet}$, with no trapped electrons) in relation to the neutral lattice. The neutral and single charged vacancies may be ionized and act as donors so that, taking into account the presence of ferrous ions in the samples, the oxygen vacancies may be described

in the form of donor complexes[42] as

$$[n\mathrm{Fe}^{3+}{*}V_{\mathrm{O}}]\Leftrightarrow[(n-1)\mathrm{Fe}^{3+}{*}\mathrm{Fe}^{2+}{*}V_{\mathrm{O}}^{\bullet}], \qquad (14)$$

$$[n\mathrm{Fe}^{3+}{*}V_{\mathrm{O}}^{\bullet}]\Leftrightarrow[(n-1)\mathrm{Fe}^{3+}{*}\mathrm{Fe}^{2+}{*}V_{\mathrm{O}}^{\bullet\bullet}], \qquad (15)$$

where the notation show that the electron moves in the coordination sphere of n iron ions surrounding the oxygen vacancy. Then the migration of these vacancies was proposed as a source of disaccommodation in YIG,[18,43,44] due to the variety of reactions involving the trapped electrons and the resulting interactions with the magnetic moments of the lattice. Therefore, the process found at higher temperatures may be related to this type of mechanism enhanced when the sintering temperature is increased. Moreover, this migration would be expected to be more complicated than a simple exponential process if we consider that these relaxation mechanisms are induced by donor complexes. The fitting of the isochronal curves for this DA process through our algorithm results in an energy distribution near 0.52 eV, very similar to the values proposed by the authors mentioned.

Nevertheless, the dynamics of the domain walls in these samples seems to be not only caused by the relaxation processes analyzed, as can be deduced from the experimental results obtained. In fact, all of the samples show a negative disaccommodation process or accommodation process in the temperature range tested. There are several reasons to analyze and understand the underlying mechanisms responsible for these phenomena.[16,18] However, the hypothesis suggested (heating of the samples, dependences with the demagnetizing field, anomalous reduction of the anisotropy due to a temporal decrease of the Fe^{2+} ion content etc.) cannot satisfactorily justify the diverse experimental features of these accommodation processes. In our point of view, two important facts must be obtained from the experimental results. First, these phenomena have only been detected in this type of ferrite sintered in reducing atmospheres, but never in others such as spinel and hexagonal ferrites. Second, these experimental results show an extreme dependence on the measurement frequency where the accommodation processes appear, but such a dependence is not found where these processes are not considerable. Therefore, it seems reasonable to relate such mechanisms to a certain characteristic property of these samples that is a function of the measurement frequency.

For these reasons, let us now consider the theoretical ideas of Sec. II relating to the dynamics of the domain walls. According to this theory, for values of the measuring frequency considerably higher than the inverse of the time constant of the relaxation process, the rearrangement of the defects is too slow to follow the domain-wall motion. Then, as this rearrangement takes place, the wall damping diminishes. Finally, when this process has ended, the defects will stay at their equilibrium positions, giving rise to an additional elastic stress over the domain wall. Therefore, taking into account a second-order wall dynamics, this stress will be increased at each time instant due to the induced anisotropy relaxation term. Hence the wall resonance frequency will be increased as a consequence in the same way, as shown in Fig. 2, according to Eq. (10). Thus the temporal evolution of the wall oscillation amplitude will depend on the measuring frequency, and then a maximum after the demagnetization stage may appear. This behavior must be confirmed with the help of the measurement of a related macroscopic magnitude, that is to say, by means of the initial permeability evolution. To this end, in Figs. 16 and 17 we plot the initial permeability curves obtained with either the measuring frequency or the temperature as a parameter, respectively. These representations, which can be obtained in the same way for the rest of the samples, are coherent with the ideas exposed above since they show a very similar behavior. Thus, for measuring frequencies lower than the wall resonance, the only phenomenon detected is the diminution of the permeability due to the induced anisotropy relaxing mechanisms.

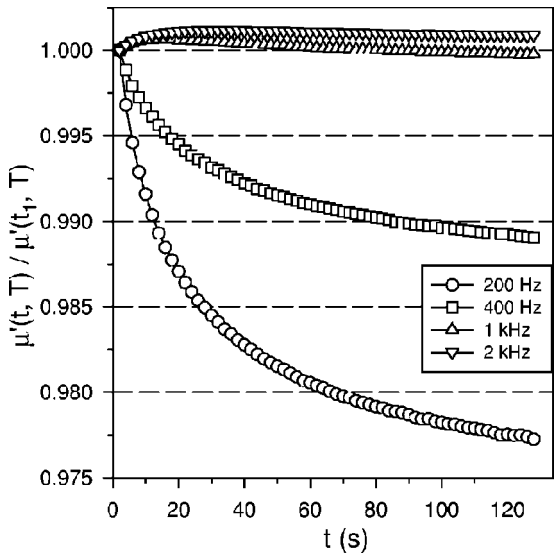

FIG. 16. Temporal evolution of the initial permeability measured at 122 K and different frequencies for the stoichiometric YIG sintered at 1420 °C in CO_2.

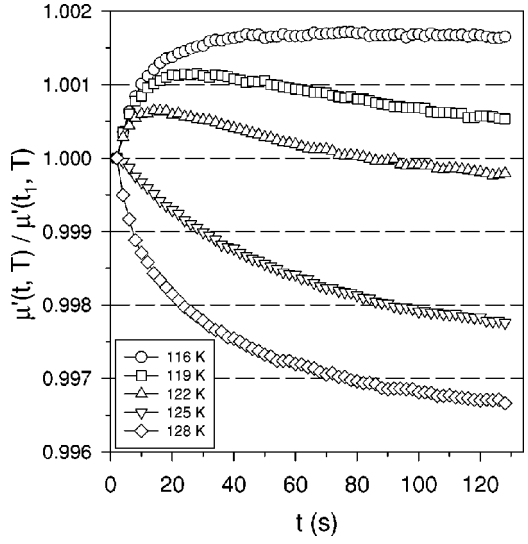

FIG. 17. Temporal evolution of the initial permeability measured at 1 kHz and different temperatures for the stoichiometric YIG sintered at 1420 °C in CO_2.

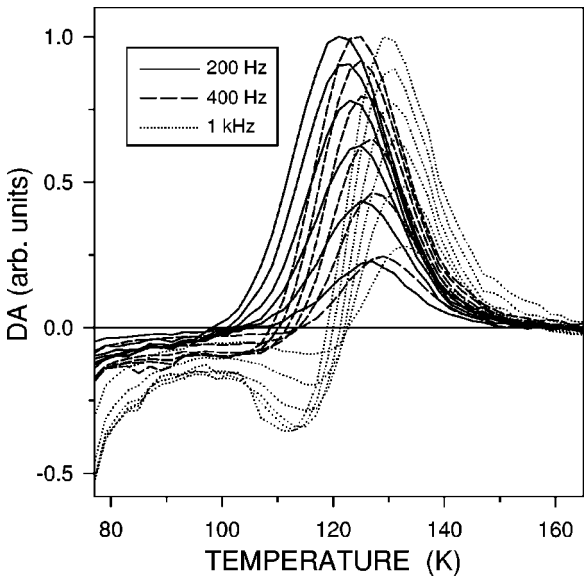

FIG. 18. Comparison between the disaccommodation and accommodation processes with increasing measurement frequencies. In order to obtain a clearer representation, the maximum value of the disaccommodation peak has been normalized for all of the frequencies.

When that frequency is increased both processes, magnetic disaccommodation and time-dependent wall resonance, take place, giving rise to the isochronal spectra constructed. These inferences are more clearly shown in Fig. 18, in this case for the YIG sample sintered at 1420 °C with a partial oxygen pressure of 10^{-2} atm. At 200 Hz one can observe the peak corresponding to process II while the accommodation process is hardly noted. As this frequency is increased we approach that of the wall resonance. When this process is noteworthy it produces a temporal increment followed by an additional decrease of the permeability that concludes in an apparent shift of the disaccommodation peak, which, obviously, does not involve a real increment of the activation energy of the process.

It is important to point out that other authors[40,45,46] proposed similar ideas in their studies of the wall mobility of polycrystalline YIG samples. In fact, the dependence of the wall damping on the measuring frequency due to the presence of defects in the lattice was proven in all these works. For high enough frequencies the diffusion of these defects is too slow to follow the wall motion, resulting in an increase of the restoring force over the wall and thus in an increase of the wall energy associated with the relaxation process. Moreover, the activation energy obtained for this process (0.27 eV) in one of these works[40] is very close to that confirmed in this paper for process II.

Finally, it must be assumed, as we previously stated, that if a resonance phenomenon takes place then the imaginary component of the permeability, related to the magnetic losses of the material, must show an abrupt variation with time in that temperature zone. In this way, the initial permeability curves (Figs. 8–12) exhibit the presence of a peak in μ'' at a temperature dependent on the frequency but in any case higher than 100 K. This peak varies strongly with time and appears at temperatures always close to the corresponding relaxation process detected in μ'. For these reasons, according to our theory, an accommodation process must be noted at these temperatures, as it can be observed in the isochronal spectra. However, the peak of μ'' around 200 K does not cause any accommodation process, because no anisotropy relaxation process is found close to it; thus it hardly depends on the time passed since the demagnetization of the sample. It must be mentioned that other authors[41] also found a peak in μ'' that shifts to lower frequencies for decreasing temperatures, in this case related to a relaxation process through an electronic diffusion characterized by an activation energy of 0.38 eV, again comparable to the values proposed in this work.

VI. CONCLUSIONS

In this work we have studied the dynamics of the domain walls by means of the analysis of the magnetic aftereffect processes in polycrystalline YIG samples. For this purpose we have measured the well-known magnetic disaccommodation showing the presence of the relaxation process related to the electronic hopping between ferric and ferrous ions in octahedral positions of the lattice (process II). At the same time, magnetic accommodation processes have been detected in all samples at temperatures immediately lower than process II. These phenomena have been described through a theoretical model which studies the dynamics of the domain walls as a function of the measuring frequency. According to this theory the origin of the accommodation process is associated with a time-dependent resonance mechanism due to the existence of an induced anisotropy relaxation process. Finally, we have successfully confirmed the correlation between our diverse experimental results and the theoretical analysis.

ACKNOWLEDGMENT

This work was partially supported by Junta de Castilla y León, Project No. VA 06/00B.

*Electronic address: ctorres@ee.uva.es

[1] O. Alejos, C. de Francisco, J.M. Muñoz, P. Hernández, and C. Torres, Phys. Rev. B **58**, 8640 (1998).
[2] L. Néel, J. Phys. Radium **13**, 249 (1952).
[3] F. Walz and H. Kronmüller, Phys. Status Solidi B **181**, 485 (1994).
[4] F. Walz, J. Rivas, D. Martínez, and H. Kronmüller, Phys. Status Solidi A **144**, 177 (1994).
[5] F. Walz, J. Rivas, J. Iñiguez, and H. Kronmüller, Phys. Status Solidi A **151**, 435 (1995).
[6] F. Walz, J. Rivas, J. Iñiguez, and H. Kronmüller, Phys. Status Solidi A **158**, 217 (1996).
[7] O. Alejos, C. de Francisco, J.M. Muñoz, P. Hernández, C. Torres, J.I. Iñiguez, and L. Torres, J. Magn. Magn. Mater. **202**, 141 (1999).
[8] F. Walz and J. Rivas, Phys. Status Solidi A **37**, 151 (1976).

[9] F. Walz, L. Torres, K. Bendimya, and C. de Francisco, Phys. Status Solidi A **164**, 805 (1997).
[10] O. Alejos, C. de Francisco, J.M. Muñoz, P. Hernández-Gómez, C. Torres, and A. González Arias, Jpn. J. Appl. Phys. **40**, 2245 (2001).
[11] P. Hernández-Gómez, K. Bendimya, C. de Francisco, J.M. Muñoz, O. Alejos, and C. Torres, J. Magn. Magn. Mater. **226-230**, 1409 (2001).
[12] O. Alejos, C. de Francisco, J.M. Muñoz, P. Hernández-Gómez, C. Torres, K. Hisatake, and I. Matsubara, IEEE Trans. Magn. **37**, 3028 (2001).
[13] P. Hernández-Gómez, K. Hisatake, C. de Francisco, J.M. Muñoz, O. Alejos, C. Torres, and I. Matsubara, J. Magn. Soc. Jpn. **23**, 2134 (1999).
[14] P. Hernández-Gómez, P.G. Bercoff, C. de Francisco, J.M. Muñoz, O. Alejos, C. Torres, and H.R. Bertorello, J. Appl. Phys. **87**, 6250 (2000).
[15] L. Torres, C. de Francisco, J.M. Muñoz, M. Zazo, and J.I. Iñiguez, J. Appl. Phys. **73**, 6301 (1993).
[16] C. Torres, C. de Francisco, L. Torres, R. de Miguel, P. Hernández, and J.I. Iñiguez, J. Phys. IV **C1**, 289 (1997).
[17] C. Torres, R. Orejudo, C. de Francisco, J.M. Muñoz, P. Hernández, O. Alejos, and L. López-Díaz, Phys. Status Solidi A **169**, 145 (1998).
[18] L. Torres, F. Walz, J. Iñiguez, and H. Kronmüller, Phys. Status Solidi A **159**, 485 (1997).
[19] F. Walz, L. Torres, J. Iñiguez, and H. Kronmüller, Phys. Status Solidi A **180**, 507 (2000).
[20] C. Torres, C. de Francisco, J.M. Muñoz, P. Hernández-Gómez, O. Alejos, P.G. Bercoff, H.R. Bertorello, and J.I. Iñiguez, Physica B (to be published).
[21] R.P. Hunt, J. Appl. Phys. **38**, 2826 (1967).
[22] A. Broese van Groenou, J.L. Page, and R.F. Pearson, J. Phys. Chem. Solids Suppl. **28**, 1017 (1967).
[23] U. Enz and H. van der Heide, J. Appl. Phys. **39**, 435 (1968).
[24] O. Alejos, Ph.D. dissertation, University of Valladolid, 1997.
[25] S. Krupicka and K. Záveta, *Anisotropy, Induced Anisotropy and Related Phenomena* (Wiley, New York, 1975).
[26] G.H.J. Wantenaar, G.V. Wilson, D.H. Chaplin, and S.J. Campbell, J. Magn. Magn. Mater. **89**, 13 (1990).
[27] K.L. Ngai, Comments Solid State Phys. **9**, 141 (1980).
[28] H.J. Van Hook, J. Am. Ceram. Soc. **45**, 162 (1962).
[29] C. de Francisco, J. Iñiguez, J.M. Muñoz, and J. Ayala, IEEE Trans. Magn. **23**, 1866 (1987).
[30] C. Torres, Ph.D. dissertation, University of Valladolid, 2001.
[31] C. Torres, O. Alejos, C. de Francisco, J.M. Muñoz, and P. Hernández-Gómez, Appl. Phys. A: Mater. Sci. Process. (to be published).
[32] G. Winkler, *Vieweg Tracts in Pure and Applied Physics: Magnetic Garnets* (Vieweg & Sohn, Braunschweig, 1981), Vol. 5.
[33] F. Walz, J.H.V.J. Brabers, L. Torres, and H. Kronmüller, Phys. Status Solidi B **228**, 717 (2001).
[34] S. Geller and M.A. Gilleo, J. Phys. Chem. Solids **3**, 30 (1957).
[35] R.P. Hunt, J. Appl. Phys. **37**, 1330 (1966).
[36] L. Torres, M. Zazo, J.I. Iñiguez, C. de Francisco, and J.M. Muñoz, IEEE Trans. Magn. **30**, 4903 (1994).
[37] R.E. Fontana and D.J. Epstein, Mater. Res. Bull. **6**, 959 (1971).
[38] T. Merceron and J. Loriers, Phys. Status Solidi A **44**, K147 (1977).
[39] J. Verweel and B.J.M. Roovers, *Solid State Physics in Electronics and Telecommunications* (Academic Press, New York, 1960), Vol. 3, p. 475.
[40] T. Merceron, M. Guyot, and V. Cagan, Phys. Lett. **95A**, 383 (1983).
[41] D.J. Epstein and B. Frackiewicz, J. Appl. Phys. **30**, 295S (1959).
[42] P.K. Larsen and R. Metselaar, Phys. Rev. B **8**, 2016 (1973).
[43] K. Hisatake, I. Matsubara, K. Maeda, H. Wakao, T. Fujihara, Y. Kawai, and K. Uematsu, J. Magn. Magn. Mater. **112**, 387 (1992).
[44] K. Hisatake, I. Matsubara, K. Maeda, Y. Kawai, and S. Lyakhimets, IEEE Trans. Magn. **30**, 975 (1994).
[45] M. Guyot, T. Merceron, and V. Cagan, J. Phys. D **16**, L93 (1983).
[46] M. Guyot, T. Merceron, and V. Cagan, J. Appl. Phys. **57**, 4180 (1985).